



# Comparison between sprinkler irrigation and natural rainfall based on droplet diameter

Maosheng Ge<sup>1</sup>, Pute Wu<sup>1</sup>, Delan Zhu<sup>1</sup> and Daniel P. Ames<sup>2</sup>

<sup>1</sup> Northwest A&F University, College of Water Resources and Architectural Engineering, Yangling, Shaanxi, 712100, China <sup>2</sup> Brigham Young University, Dept. of Civil and Environmental Engineering, Provo, Utah, 84602, USA

## Abstract

An indoor experiment was conducted to analyze the movement characteristics of different sized droplets and their influence on water application rate distribution and kinetic energy distribution. Radial droplets emitted from a Nelson D3000 sprinkler nozzle under 66.3, 84.8, and 103.3 kPa were measured in terms of droplet velocity, landing angle, and droplet kinetic energy and results were compared to natural rainfall characteristics. Results indicate that sprinkler irrigation droplet landing velocity for all sizes of droplets is not related to nozzle pressure and the values of landing velocity are very close to that of natural rainfall. The velocity horizontal component increases with radial distance while the velocity vertical component decreases with radial distance. Additionally, landing angle of all droplet sizes decreases with radial distance. The kinetic energy is decomposed into vertical component and horizontal component due to the oblique angles of droplet impact on the surface soil, and this may aggravate soil erosion. Therefore the actual oblique angle of impact should be considered in actual field conditions and measures should be taken for remediation of soil erosion if necessary.

**Additional key words:** droplet size; velocity; landing angle; kinetic energy

**Abbreviations used:** CCD (charge coupled device); DSD (drop size distribution); SP (specific power); 2DVD (two-dimensional video distrometer)

**Citation:** Ge, M. S.; Wu, P.; Zhu, D.; Ames, D. P. (2016). Comparison between sprinkler irrigation and natural rainfall based on droplet diameter. Spanish Journal of Agricultural Research, Volume 14, Issue 1, e1201. <http://dx.doi.org/10.5424/sjar/2016141-8076>.

**Received:** 26 May 2015. **Accepted:** 16 Feb 2016

**Copyright © 2016 INIA.** This is an open access article distributed under the terms of the Creative Commons Attribution-Non Commercial (by-nc) Spain 3.0 Licence, which permits unrestricted use, distribution, and reproduction in any medium, provided the original work is properly cited.

**Funding:** Project of Native Sci-technology Support (2011BAD29B02); Research Center of Native Engineering Technology (2011FU125Z27-1); and 111 Project of Chinese Education Ministry (B12007).

**Competing interests:** The authors have declared that no competing interests exist

**Correspondence** should be addressed to Pute Wu: [gjzwpt@vip.sina.com](mailto:gjzwpt@vip.sina.com)

## Introduction

Distinct differences exist in the formation, size distribution, and movement of water droplets emitted from sprinkler irrigation systems versus natural precipitation water droplets. In the case of sprinkler irrigation, a water jet breaks into droplets as it is sprayed through a nozzle at a specified angle while natural rain is generally generated in high altitude clouds and falls mostly perpendicular to the earth surface. Water droplets formed and moving in such distinct ways are likely to exert different effects on the surface soil. Droplet size distribution (DSD) impacts water and energy distribution, soil water infiltration rate, and soil erosion. Therefore it is important to understand the breakup of the water jet, droplet velocity distribution, and kinetic en-

ergy to the soil from the perspective of particle sizes when using sprinkler irrigation technology and its comparison with characteristics of natural rainfall.

Many researchers have studied the distribution of drop sizes in sprinkler irrigation (e.g. Solomon *et al.*, 1985; Kincaid *et al.*, 1996; McCreery *et al.*, 1996; Montero *et al.*, 2003; Nuyttens *et al.*, 2007), and the results show that the drop sizes distribution is affected by the nozzle size and working pressure. Kincaid *et al.* (1996) found the ration of nozzle size to working pressure to be a useful parameter in characterizing drop size distribution for sprinklers. Both Kincaid *et al.* (1996) and Montero *et al.* (2003) found that working pressure has the most significant influence on drop sizes. Salvador *et al.* (2009) described a low-speed imaging method to determine the size and velocity of

spray irrigation water droplets; because each measuring location had very few droplets, it was difficult to fully characterize the distribution of sizes at each location. King *et al.* (2010) developed an improved laser-based sensor fixed on a hinged bracket, which can be adjusted to guarantee rainfall pass-through in the test area along normal direction. In the study of rainfall kinetic energy, specific power (SP) is a commonly used indicator to explain surface runoff and soil erosion. Thompson & James (1985) and Mohammed & Kohl (1987) found soil water infiltration before the generation of surface runoff decreases with increase of SP. Thompson *et al.* (2001) indicated that sediment yield is linearly related to SP during rainfall. King & Bjorneberg (2010) compared four commonly used sprinkler nozzles including I-Wob, Nelson D3000, R3000, and S3000 and the results showed that Nelson D3000 nozzle produces a maximum SP. Calculation of SP requires measurement or estimation of both the size and velocity of the droplet. Although King *et al.* (2010) measured the actual velocity using a laser-based sensor, the components of the velocity in vertical and horizontal directions were not considered. Additionally, the effects caused by horizontal and vertical kinetic energy on the ground could not be estimated. Others have studied the movement of natural rainfall and proposed various experimentally based models to define this movement (Laws & Parsons, 1943; Gunn & Kinzer, 1949; Atlas & Ulbrich, 1977; Ulbrich 1983).

This paper presents a study of the raindrop size and shape spectrum with respect to radial distance during sprinkler irrigation. Droplet velocity, landing angle and kinetic energy were measured together with droplet diameter and then compared with those of natural rainfall. The results are helpful for adequate irrigation for different types of soil under sprinkler irrigation and to help avoid soil erosion.

## Material and methods

### Sprinkler nozzle

For this study, a Nelson D3000 (Nelson Irrigation Corp., Walla Walla, WA, USA) sprinkler nozzle with a 4.76 mm diameter and a strike plate with 36 grooves was used (Fig. 1). Both nozzle size and working pressure have impact on the droplet size distribution and the influence from working pressure seems to be more significant (Kincaid *et al.*, 1996; Montero *et al.*, 2003), so the working pressures were set as 66.3 kPa, 84.8 kPa, and 103.3 kPa in our research. Water flows out of the nozzle and is dispersed into a single water jet after hitting on the plate.



**Figure 1.** Sprinkler nozzle and plate used in the experiment.

### Indoor test device

The test was carried out using a sprinkler test platform in the irrigation hydraulics experiment station at Northwest Agriculture and Forestry University, Yangling, China (Fig. 2). The nozzle was installed perpendicular to the ground at a height of 2 m. A CYB131 pressure transmitter produced by Xi'an Xinmin Electronics Co., Ltd. (range 0-0.6 MPa, accuracy of 0.1%, the output signal 4-20 mA) was situated 0.2 m above the nozzle. Flow rates were measured using an EMF5000 electronic flow meter (range 0.2895-28.95 m<sup>3</sup>/h), a centrifugal pump of 2.2kW was selected and the upstream reservoir volume was 20 m<sup>3</sup>.

### Test and calculation methods

*Sprinkler application rate test.* The grooved flow channels of the D3000 spread irrigation water into dozens of single water jets and each water jet is relatively independent (Clark *et al.*, 2003). The water jet was captured in a HOBO RG3-M self-recording rain barrel-type catch-can (1% accuracy, resolution 0.02 mm) with a height of 25.7 cm, and the inner and outer diameters were 15.2 cm and 17 cm respectively. Forty-five catch-cans were arranged in a line leading away from the sprinkler with a spacing of 17 cm. Each measurement lasted 1 hour and was repeated 3 times.

*Droplet size and velocity test.* A two-dimensional video distrometer (2DVD) produced by Joanneum Research (Austria) was used to measure droplet size and velocity. Two vertically disposed CCD cameras inside the instrument make a linear scan of raindrops passing through the test area and record the precipitation rate, individual drop size, and vertical and horizontal velocity components. The minimum drop size available is 0.19 mm and the measuring scope is 100×100 mm<sup>2</sup>. The 2DVD was placed along the radial

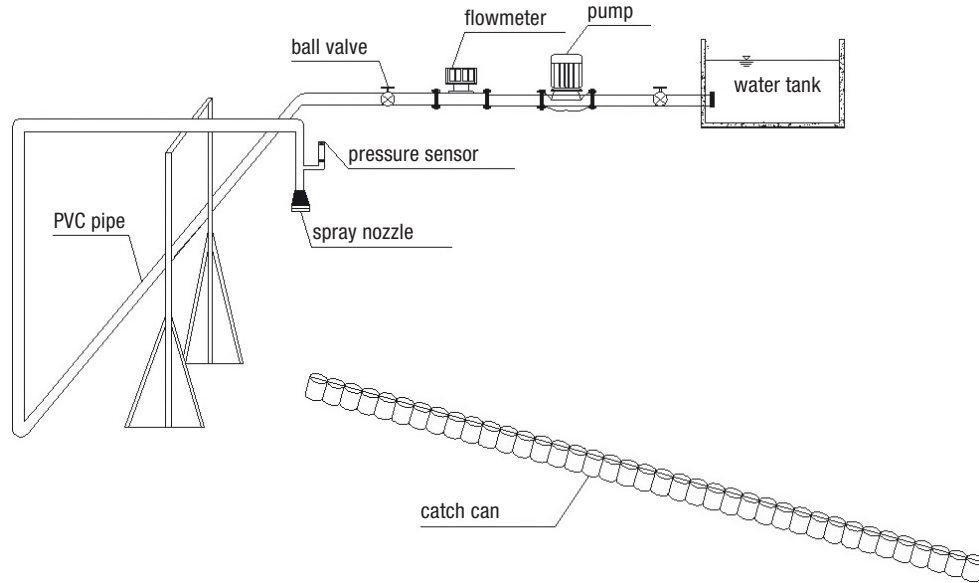


Figure 2. Layout of the test platform.

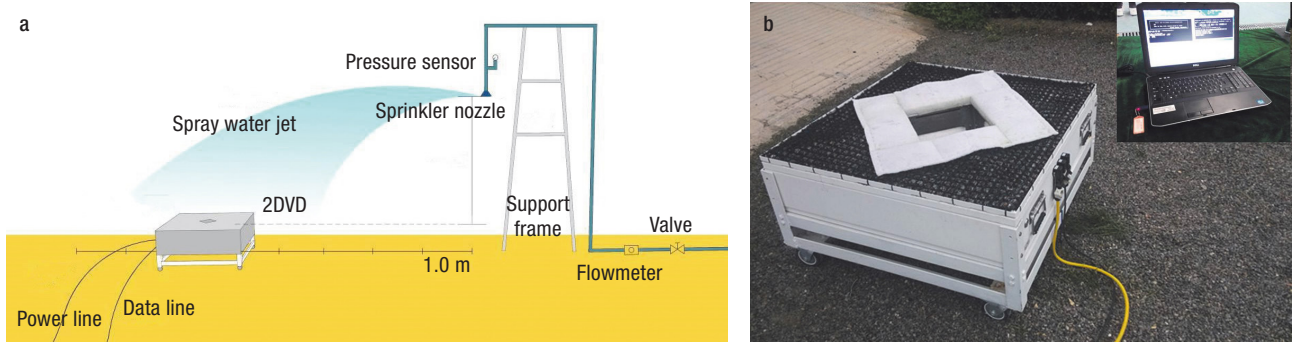


Figure 3. Layout of droplet diameter and velocity test platform: schematic diagram of indoor test platform for sprinkler (a) and the outdoor natural rainfall test device (b).

direction of water jet (Fig. 3a) with spacing between measuring points at 1 m and with each measurement lasting 3 minutes. The droplet size and velocity of natural rainfall was also measured using the 2DVD placed outdoors without any shelter (Fig. 3b).

**Droplet landing angle.** The trajectory of sprinkler droplets is shown schematically in Fig. 4. Droplets leave the sprinkler plate at an angle of  $\theta$  and land on the horizontal surface at a speed of  $V_t$  after a period of time. The angle  $\beta_0$  between  $V_t$  and horizontal plane is called landing angle. The horizontal velocity  $V_{tx}$  and vertical velocity component  $V_{ty}$  of a single drop are computed directly by the 2DVD. Therefore the landing angle can be obtained through inverse tangent of the ratio of  $V_{ty}$  and  $V_{tx}$ .

**Specific power.** Eqs. [1]-[3] are used to compute SP and its directional components (Erpul *et al.*, 2008):

$$SP = \left[ k \sum_{i=1}^n d_i^3 v_i^2 \right] A^{-1} t^{-1} \quad [1]$$

$$SP_x = SP \cos \beta_0^2 \quad [2]$$

$$SP_y = SP \sin \beta_0^2 \quad [3]$$

where  $SP$  is the specific power ( $J/m^2/s$ ),  $d_i$  is the size of the droplet (mm);  $v_i$  is the velocity of the droplet (m/s);  $n$  is the number of droplets pass through the test area;  $A$  is the test area ( $mm^2$ );  $t$  is the measuring time (s);  $k$  is the conversion constant;  $SP_x$  and  $SP_y$  are the components of  $SP$  in the direction of X axis and Y axis ( $J/m^2/s$ ); and  $\beta_0$  is the landing angle of droplet ( $^\circ$ ).

### Movement characteristics of natural rainfall

**Calculation of droplet velocity.** Natural raindrops fall under the influence of air resistance. When air resistance is equal to its own gravity, raindrops reach a steady fall velocity, which is also called the terminal velocity. This velocity relates to each drop's size and shape. A number of equations have been derived from

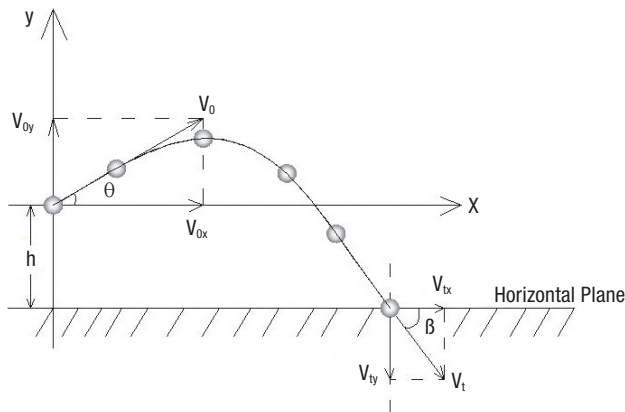


**Figure 4.** Schematic diagram of sprinkler droplets trajectory.

test data for estimating terminal velocity. The most commonly used form is the power function (Atlas & Ulbrich, 1977; Ulbrich, 1983):

$$u_T(D) = \alpha D^\beta \quad [4]$$

where  $\mu T(D)$  is the terminal velocity (m/s);  $\alpha$  and  $\beta$  are calibration coefficient with typical values of 3.778 and 0.67 respectively (Atlas & Ulbrich, 1977); and  $D$  is the droplet diameter (mm).

To validate the accuracy and applicability of Equation [4] in the local rainfall, three natural rainfall tests were conducted using the 2DVD at a test site as shown in Fig. 3b. Wind speed during the rainfall tests did not exceed 3 m/s.

*Natural rainfall droplet size distribution.* Equation [5] (Ulbrich, 1983) was used to estimate raindrop size distribution:

$$N'(D) = \alpha N_0 D^{\beta+\mu} e^{-\Lambda D} \quad [5]$$

where  $N_0$  is a constant approximately equal to  $8.0 \times 10^3$ ;  $\alpha$  and  $\beta$  are the same calibration coefficients as in Eq. [4];  $\mu$  is the raindrop shape factor associated with rainfall type,  $0 \leq \mu \leq 1$ ; and  $\Lambda$  is a power function related to rain application rate  $I$  (mm/h),  $\Lambda = 4.13I^{-0.21}$  (Beard, 1976).

## Results and discussion

### Droplet size distribution

The rain application rate and composition of drop size of the Nelson D3000 sprinkler nozzle under pressures of 66.3 kPa, 84.8 kPa and 103.3 kPa are shown in Table 1 and Fig. 5. Although there is a large difference in application rate between the radial measuring points, especially at the point of  $L=4.2$  m (where the

**Table1.** Application rate (mm/h) of each point along radial direction of D3000 ( $L$  is the distance from the nozzle to the measuring point).

L (m)	Pressure (kPa)		
	66.3	84.8	103.3
1.0	1.2	4.8	0.33
2.0	0.6	3	0.48
3.0	0.6	2.4	0.46
3.5	3.0	2.4	0.60
4.0	33.1	12	1.47
4.2	190.8	24	3.31
4.4	153.7	105.6	7.65
4.5	133.5	144.3	9.59
4.6	0	172.8	10.65
4.8	0	27.6	33.6
5.0	0	0	77.40
5.5	0	0	122.34
5.8	0	0	96.09
6.0	0	0	13.37
6.2	0	0	0

application rate reaches 190 mm/h), there is still evident regularity in the droplet size composition. Each measuring point exhibits a clear distribution of droplet sizes. The size distribution range becomes narrower and the average droplet size becomes smaller when the distance between test point and nozzle gets shorter. The droplet size with the largest frequency also shares a larger proportion when the distance between test point and nozzle is close, and vice versa. The composition of drop size of each measuring point along the radial direction under pressure 84.8 and 103.3 kPa is shown in Figs. 5b and 5c. Both figures reflect exactly the same drop size composition with that of Fig. 5a. Additionally, Fig. 5 shows that with increasing pressure at the nozzle, the number of droplets with a size smaller than 0-0.5 mm diameter increases significantly.

The natural raindrop size distribution measured by raindrop spectrometer is shown in Fig. 6a. Eq. [5] was used to calculate the raindrop size distribution with the same measured application rate. Comparison of the two cases shows that the drop size distributions pattern are highly consistent. The number of droplets with the size of 0.4-1 mm accounts for more than 60% of the total droplets. The measured proportion of droplets with the sizes of 0.4-0.6 mm are slightly higher than that of the calculated value, which maybe was mainly caused by the accuracy of raindrop shape factor  $\mu$ . Fig. 6b shows the raindrop size distribution of 1, 10 and 100 mm/h application rate based on Eq. [5]. Precipitation intensity per unit time and per unit area increases with increased application rate. There is also a significant increase in the proportion of large droplets.

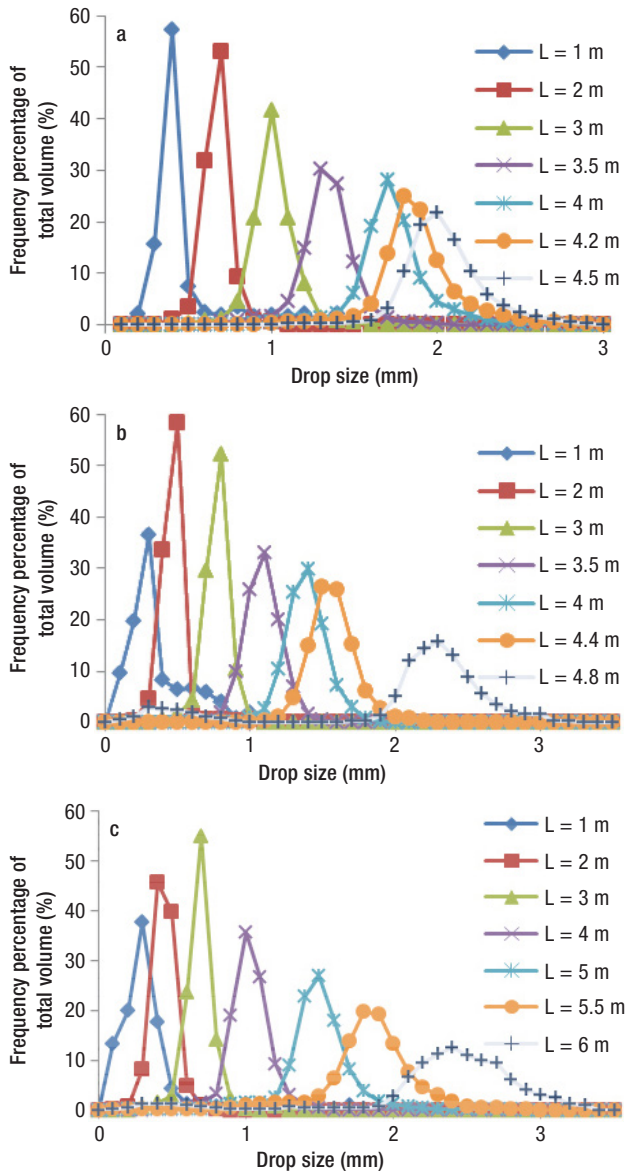


**Figure 5.** Composition of the drop size under three pressures of D3000: P = 66.3 kPa (a), P = 84.8 kPa (b) and P = 103.3 kPa (c). L is the distance from the nozzle to the measuring point.

Comparing the droplet size composition of sprinkler irrigation and with that of natural rainfall conditions shows that the composition of droplet size had no obvious relation with the application rate under sprinkler conditions, but relates to the distance between measuring point and nozzle. As seen in Fig. 5, with the increase of distance between the measuring point and nozzle, the average size becomes larger and the size range becomes broader. The composition of droplet size under natural rainfall conditions mainly relates to the application rate. The proportion of relative large droplets increases with the increase of application rate. This is possibly because the raindrop size distribution for sprinkler irrigation is along the radial direction of a single nozzle, while the control area under natural rainfall is much larger.

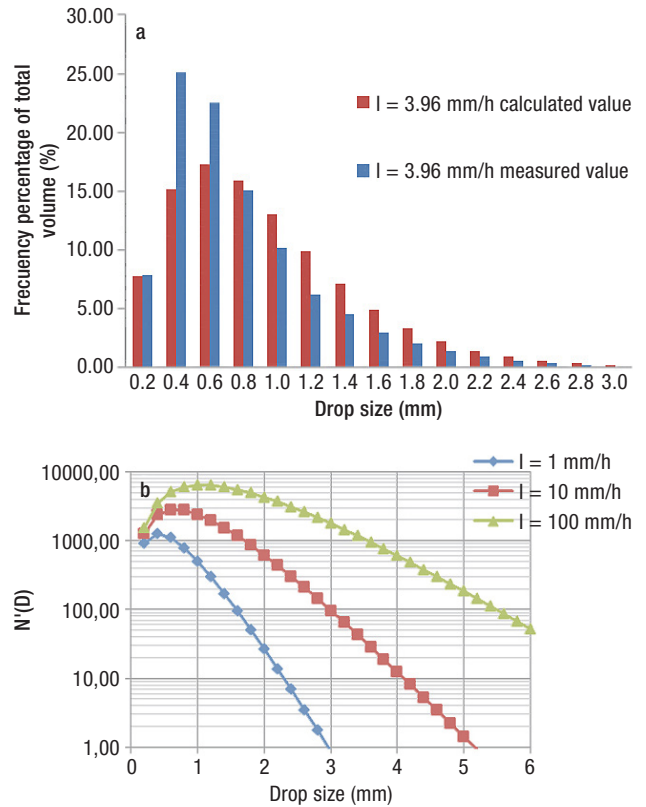


**Figure 6.** A comparison of the droplet size composition between calculated value and measured value of natural rainfall (a); calculated values of droplet size composition under three different application rates, I=1, 10 and 100 mm/h (b). I is the rainfall intensity.

### Droplet velocity distribution

The terminal velocity of each drop size obtained from the droplet spectrum analysis was compared with the terminal velocity calculated by Eq. [4]. The calibration coefficients  $\alpha$  and  $\beta$  were modified to 0.3732 and 0.848 by fitting the measured terminal velocities of raindrops. Fig. 7 shows the calculated terminal velocities of droplets with diameters of 1, 1.2, 1.4, 1.6, 1.8, and 2 mm using the revised Eq. [4].

As shown in Fig. 8, the velocity of each raindrop diameter shows an overall trend of decreasing firstly and then increasing. At the area close to the nozzle, the velocities of droplets under sprinkler irrigation are close to those of the droplets with the same drop sizes under natural rainfall. The spray droplets velocities then decrease with radial distance. These velocities are slightly lower than the terminal velocities of natural rainfall droplets, and the maximum velocity difference is 17.2% of natural rainfall terminal velocity (3.5 m to the nozzle of 1 mm drop size). Eventually, the spray droplet velocities begin to increase and approach natural rainfall terminal velocity. Generally, the difference between droplet velocities for the same drop size between sprinkler irrigation and natural rainfall is not

significant. In other words, although the two types of water droplets are generated in different ways, they reach almost the same velocity and kinetic energy when they impact on the ground.

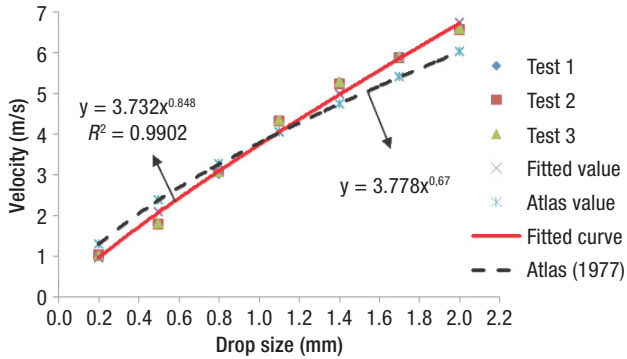


**Figure 7.** Measured and calculated values of natural rainfall closing velocity. The dashed line is the power function of drop-let velocity put forward by Atlas & Ulbrich (1977).

For further analysis of velocity change in a radial direction for each drop size, the velocity components in horizontal and vertical directions are also plotted in Fig. 8. Figure 8 shows that the vertical component of velocities along radial direction decreases while the horizontal velocity component increases. When  $d=1, 1.2$  and  $1.4$  mm, component velocities change dramatically. The vertical velocity is much higher than the horizontal velocity when close to the nozzle. While the horizontal velocity increases when the distance from the nozzle gets larger. For droplets with sizes of  $1.6, 1.8$  and  $2$  mm, the falling and rising trend of the component velocities are relatively steady, and the vertical velocity is also higher than the horizontal velocity when the droplets are close to the nozzle and tend to be equivalent at the position distant from the nozzle. Thus, although the velocity of raindrops under sprinkler irrigation is close to that of natural rainfall, the velocity

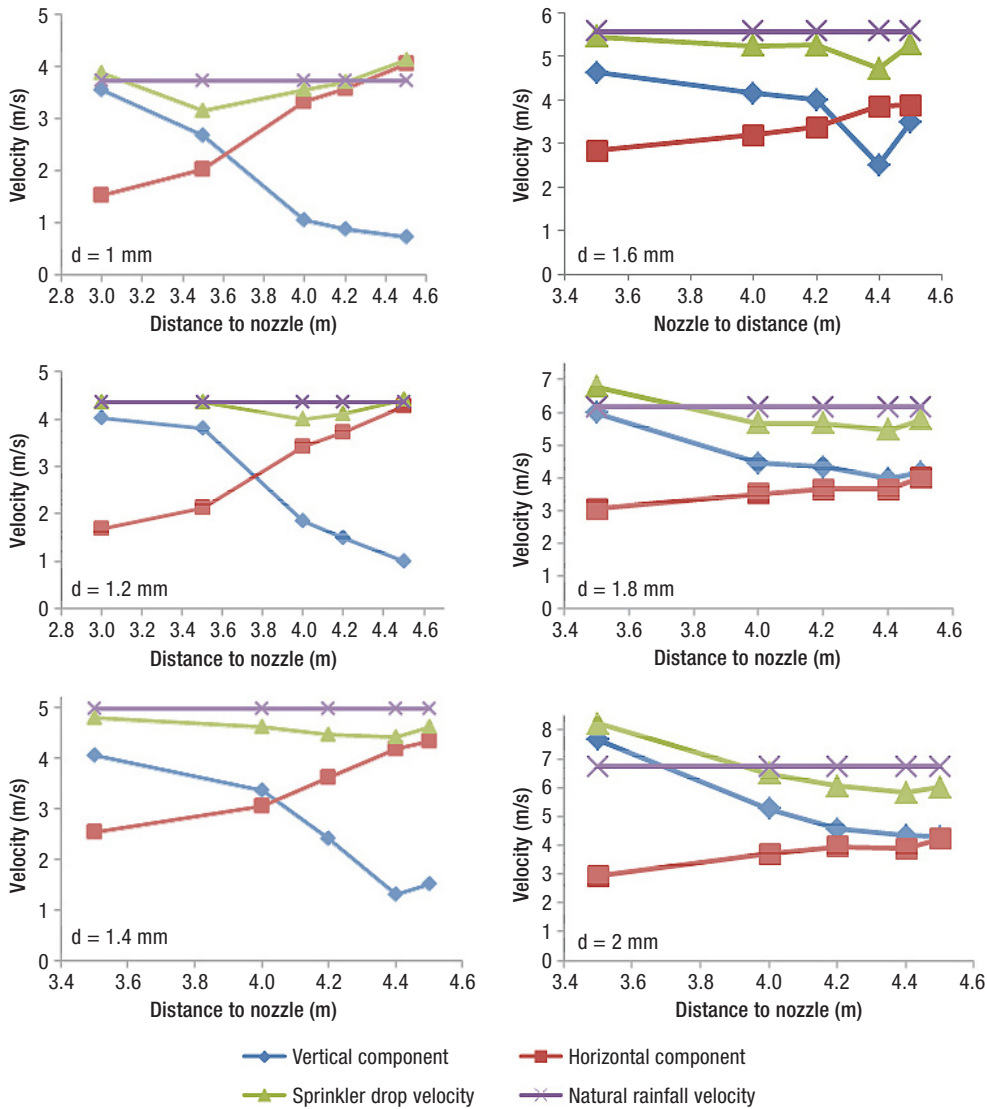


**Figure 8.** Distribution of droplets velocity and its components in horizontal and vertical directions under sprinkler irrigation and its comparison with natural rainfall;  $d$  is the droplet diameter.

components of sprinkler irrigation droplets have significant changes in the radial direction.

### Droplet landing angle distribution

Fig. 9 shows the landing angles of droplets with various sizes and locations. With the increase of the distance between test points to the nozzle, the landing angles of droplets of each size decreases. When  $d=1, 1.2$  and  $1.4$  mm, water droplets' landing angles decrease more gently and reduce from the  $60\text{-}70^\circ$  to  $40\text{-}50^\circ$ , in contrast, when  $d=1.6, 1.8$ , and  $2$  mm, water droplets' landing angles decrease more dramatically, from the  $60\text{-}70^\circ$  to  $10\text{-}20^\circ$ . The landing angles of droplets of different sizes show significant differences. This is primarily because for droplets  $d=1, 1.2$ , and  $1.4$  mm, there is a steep fall of the landing angles at a distance of  $4$  m from the nozzle, namely the vertical velocity of the droplet decreases rapidly while the horizontal velocity increases rapidly, which is also illustrated in Fig. 8. For  $d=1.6, 1.8$ , and  $2$  mm, drop landing angles produce no significant drop, showing an almost linear trend. The raindrop spectrum measured by the 2DVD shows that the landing angles of  $1\text{-}2$  mm raindrops stay between  $83\text{-}87^\circ$  under weak wind or no wind conditions, essentially vertical landing.

### Sprinkler droplets movement characteristic of precipitation concentration

Previous studies of the Nelson D3000 nozzle showed a positive relationship between SP and water application rate (Faci *et al.*, 2001; King & Bjorneberg, 2010). Under water pressures of  $66.3, 84.8$ , and  $103.3$  kPa, the maximum rates reached  $190.8, 172.8$ , and  $122.3$  mm/h, located  $4.2, 4.6$ , and  $5.5$  m from the nozzle, respectively. To explore this relationship, a detailed analysis of the spectrum at these three measuring points was made.

The raindrop distributions at  $4.2, 4.6$ , and  $5.5$  m from the nozzle are shown in Fig. 10. Fig. 10a shows that the raindrop sizes are mostly smaller than  $3$  mm under three working pressures and mainly fall with in the  $0\text{-}0.5$  mm and  $1.4\text{-}2.2$  mm size ranges. Fig. 10b shows the volume percentage of each particle size of droplet. Droplets in the range of  $1.5\text{-}2.2$  mm account for over  $90\%$  to the total volume. Although the number of droplets with size less than  $0.5$  mm is quite large, their contribution to total volume is little due to their small size. Fig. 10c shows the relationship between droplet size and landing velocity under sprinkler irrigation. Landing velocity increases with increase in drop size, following the power function Eq. [4]. Fig. 10d shows the average landing angle for each corresponding size. It can be seen from the figure that with the increase of drop size, the landing angle decreases firstly and then increases. Particles with size greater than  $1.5$  mm land at  $50^\circ$ . This trend relates to the fragmentation process of droplet. The process of precipitation droplet fragmentation is complicated. Generally it includes filamentous and sheet break up caused by the turbulent kinetic energy of the gas-liquid interface of the water jet (Testik & Barros, 2007), self-fragmentation of single large droplet (Villermaux & Bossa, 2009) or colliding and sputtering fragmentation of different sizes of droplets (Low & List, 1982), etc.

To further explore the fragmentation process of sprinkler droplets of different sizes, the landing angle of droplets with diameters of  $0.2, 0.4, 1.0, 1.4, 1.6$  and  $2.0$  mm measured at the point  $4.2$  m away from the nozzle with a water pressure of  $66.3$  kPa are plotted in Fig. 11. Figure 11 illustrates the variation of landing angle by droplet size with two obvious transition diameters ( $d=0.4$  mm and  $d=1.4$  mm). The landing angle range of transition diameters is large, which is due to the fact that the horizontal and the vertical component of velocity have no obvious regularity. This shows that raindrops may generate from a variety of fragmentation methods and the fragmentation process has a strong randomness.

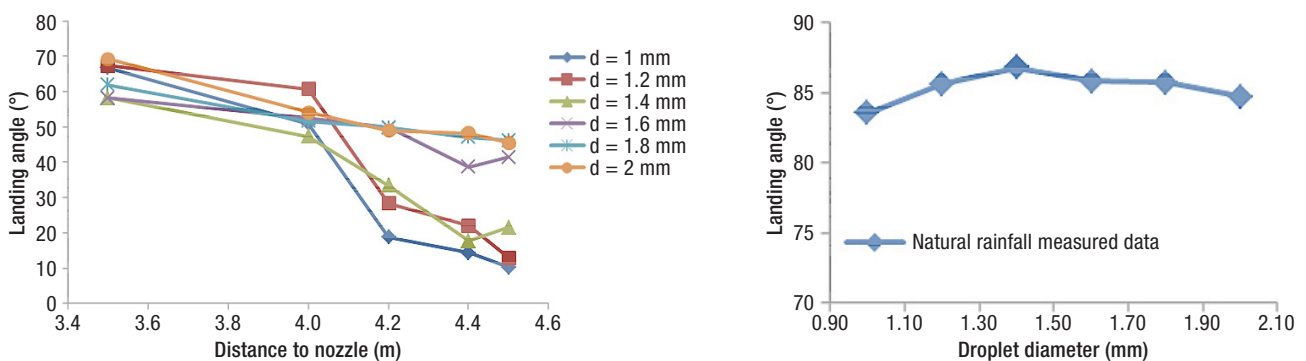


**Figure 9.** Droplets landing angle distribution of various sizes and locations under sprinkler irrigation and natural rainfall;  $d$  is the droplet diameter.

Droplets with particle size of 0.2 mm generally land perpendicularly. In addition to a small amount of small droplets generated just before landing, the majority of droplets of this size reach a balanced force and descend at an even velocity. Droplets with particle size of 1.6 and 2.2 mm hit the ground at 50°. Fig. 10b shows that the value of 1.6-2.2 mm diameter droplets reaches to a high proportion of the total volume of spray irrigation. These droplets break up directly from the mainstream under the influence of turbulent kinetic energy on the two-phase flow interface and fall on the ground soon after fragmentation, so these droplets basically followed the incident direction of the mainstream jet.

### Kinetic energy analysis of sprinkler droplets of precipitation concentration

Kinetic energy is a key indicator to measure the impact strength of the raindrops on the surface soil.

High kinetic energy can cause surface soil erosion and loss and form tiny gullies, which seriously affect the quality of arable land. The mainstream jet landing angle does not change with the changing of nozzle outlet pressure from Fig. 10d, and the mainstream jet landing angle under this test condition is 50°. SP and its components in horizontal and vertical directions at the three measuring points noted above were calculated according to Eqs. [1]-[3], and the results are shown in Table 2. The data in the table shows that the extreme value of SP under this experimental condition was more than 0.5 J/m<sup>2</sup>/s and the component SP in the horizontal direction is slightly less than that in the vertical direction and the ratio is 0.704. Comparing these data with natural rainfall data in windy conditions simulated by Erpul *et al.* (2008), it is found that the energy distribution in this study are close to the data under the condition of working pressure of 100 kPa and 150 kPa, with a 6.4 m/s wind speed. In Erpul's trial, the amounts of sediment formation under the above conditions are very

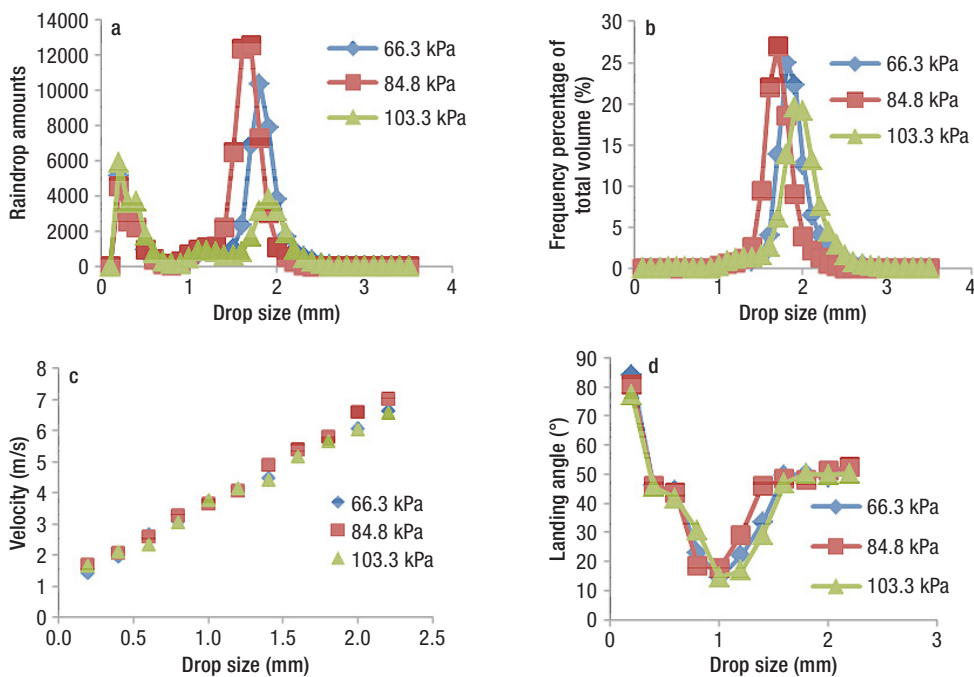


**Figure 10.** Rain drop spectrum of three measuring points with the highest application rates, which are 4.2 m to the nozzle under 66.3 kPa, 4.6 m to the nozzle under 84.8 kPa and 5.5 m to the nozzle under 103.3 kPa: droplet number of each drop size (a); proportion of total volume of each drop size (b); average velocity of each drop size (c); and landing angle of each drop size (d).

**Table 2.** Specific power (SP) and its components in horizontal and vertical directions.

Data source	P (kPa)	$\beta_0$ (°)	SP (J/m <sup>2</sup> /s)	SP <sub>x</sub> (J/m <sup>2</sup> /s)	SP <sub>z</sub> (J/m <sup>2</sup> /s)	SP <sub>x</sub> /SP <sub>z</sub>
This study	68.4	50	1.003	0.414	0.589	0.704
	84.8	50	0.869	0.359	0.51	0.704
	103.3	50	0.593	0.245	0.348	0.704
Erpul <i>et al.</i> (2008)	100	55	0.422	0.219	0.203	0.93
	150	55	0.41	0.213	0.197	0.92

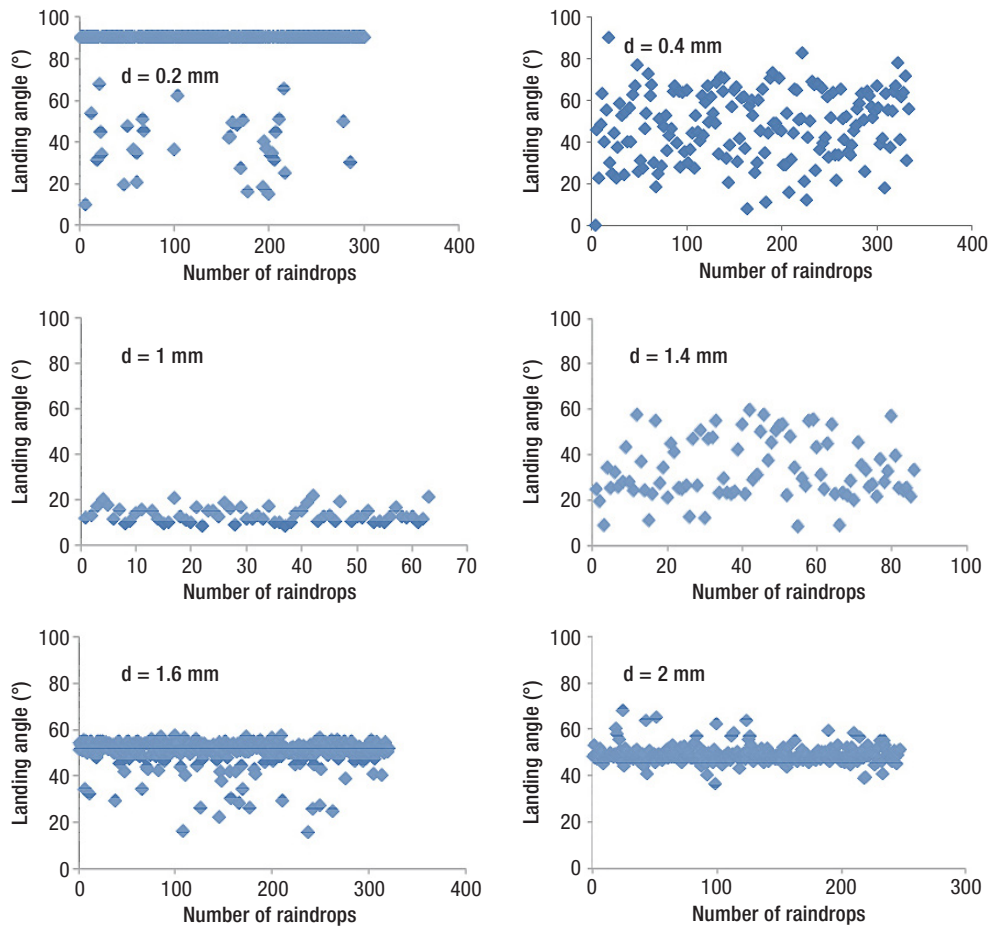


**Figure 11.** Droplet landing angle of each size at the point 4.2 m to the nozzle under 66.3 kPa;  $d$  is the droplet diameter.

high, reaching 54.58 and 44.49  $\text{g}/\text{m}^2/\text{min}$ , respectively, which indicates severe erosion according to the erosion modulus. The effects of  $\text{SP}_x$  on sediment yield were much higher than that of  $\text{SP}_y$ .

Influenced by the condition of falling height and flow angle of initial velocity, the landing angles of spray droplets do not typically reach 90 degrees. This situation is similar to natural rainfall on a sloped surface. For the vertical landing natural rainfall, surface soil is mainly affected by the vertical force. The impact of the force on the surface soil leads to a compaction effect and reduces soil porosity, and the soil infiltration rate decreases eventually. Under sprinkler irrigation raindrops often fall on the ground in an inclined angle, and the surface soil receives forces both in the vertical and horizontal directions. In the past research on sprinkler irrigation kinetic energy, the influence of soil caused by the energy components generally was not taken into consideration, what lead to the lack of understanding of the differences between natural precipitation and irrigation precipitation. In fact, due to the actual production process, it is easier to cause greater soil erosion and migration under sprinkler ir-

rigation, especially in sandy loam and silt loam. So, when using sprinkler irrigation on various types of soil, appropriate nozzle types and reasonable irrigation application rates should be selected. In addition, appropriate sprinkler installation height or slightly increased mainstream water jet angles can be helpful in reducing the effects of sprinkler irrigation on soil erosion.

In summary, in this study, the radial droplets spectrum of D3000 sprinkler nozzle was measured and compared with that of natural rainfall from the perspective of droplet velocity, landing angle and kinetic energy. The comparison indicates that the spray performance of each individual droplet is mainly affected by drop size and distance to the nozzle. The deviation of kinetic energy between sprinkler irrigation and natural rainfall is not obvious, however, the inclined landing angle of sprinkler irrigation give rise to a shear effect on surface soil and might increase soil erosion, especially in sandy loam and silt loam. Farm managers need to consider the nozzle types and application rates carefully when using sprinkler irrigation on various types of soil. This study is limited to indoor spraying test, outdoor tank test and field test should be carried out in

further research. Soil erosion potential of outdoor sprinkler irrigation combined with natural rainfall should be evaluated to further optimize irrigation quality.

## References

- Atlas D, Ulbrich CW, 1977. Path-and area-integrated rainfall measurement by microwave attenuation in the 1-3 cm band. *J Appl Meteorol* 16 (12): 1322-1331. [http://dx.doi.org/10.1175/1520-0450\(1977\)016<1322:PAIRM>2.0.CO;2](http://dx.doi.org/10.1175/1520-0450(1977)016<1322:PAIRM>2.0.CO;2)
- Beard KV, 1976. Terminal velocity of cloud and precipitation drops aloft. *J Atmos Sci* 33 (5): 851-864. [http://dx.doi.org/10.1175/1520-0469\(1976\)033<0851:TVA SOC>2.0.CO;2](http://dx.doi.org/10.1175/1520-0469(1976)033<0851:TVA SOC>2.0.CO;2)
- Clark GA, Srinivas K, Rogers DH, Stratton R, Martin VL, 2003. Measured and simulated uniformity of low drift nozzle sprinklers. *T ASAE* 46 (2): 1-18. <http://dx.doi.org/10.13031/2013.12983>
- Erpul G, Gabriëls D, Cornelis WM, Samray HN, Guzelordu T, 2008. Sand detachment under rains with varying angle of incidence. *Catena* 72 (3): 413-422. <http://dx.doi.org/10.1016/j.catena.2007.07.008>
- Faci JM, Salvador R, Playán E, Sourell H, 2001. Comparison of fixed and rotating spray plate sprinklers. *J Irrig Drain Eng* 127(4): 224-233. [http://dx.doi.org/10.1061/\(ASCE\)0733-9437\(2001\)127:4\(224\)](http://dx.doi.org/10.1061/(ASCE)0733-9437(2001)127:4(224))
- Gunn R, Kinzer GD, 1949. The terminal fall velocity for water droplets in stagnant air. *J Meteor* 6(4): 243-248. [http://dx.doi.org/10.1175/1520-0469\(1949\)006<0243:TTVOFF>2.0.CO;2](http://dx.doi.org/10.1175/1520-0469(1949)006<0243:TTVOFF>2.0.CO;2)
- Kincaid DC, Solomon KH, Oliphant JC, 1996. Drop size distributions for irrigation sprinklers. *T ASAE* 39 (3): 839-846. <http://dx.doi.org/10.13031/2013.27568>
- King BA, Bjorneberg DL, 2010. Characterizing droplet kinetic energy applied by moving spray-plate center-pivot irrigation sprinklers. *T ASABE* 53 (1): 137-145. <http://dx.doi.org/10.13031/2013.29512>
- King BA, Winward TW, Bjorneberg DL, 2010. Laser precipitation monitor for measurement of drop size and velocity of moving spray-plate sprinklers. *Appl Eng Agric* 26 (2): 263-271. <http://dx.doi.org/10.13031/2013.29551>
- Laws JO, Parsons DA, 1943. The relation of raindrop-size to intensity. *Trans Am Geophys Union* 24 (2): 452-460. <http://dx.doi.org/10.1029/TR024i002p00452>
- Low TB, List R, 1982. Collision, coalescence and breakup of raindrops. Part I: Experimentally established coalescence efficiencies and fragment size distributions in breakup. *J Atmos Sci* 39 (7): 1591-1606. [http://dx.doi.org/10.1175/1520-0469\(1982\)039<1591:CCABOR>2.0.CO;2](http://dx.doi.org/10.1175/1520-0469(1982)039<1591:CCABOR>2.0.CO;2)
- McCreery GE, Stoots CM, 1996. Drop formation mechanisms and size distributions for spray plate nozzles. *Int J Multiphase Flow* 22 (22): 431-452. [http://dx.doi.org/10.1016/0301-9322\(95\)00086-0](http://dx.doi.org/10.1016/0301-9322(95)00086-0)
- Mohammed D, Kohl RA, 1987. Infiltration response to kinetic energy. *T ASAE* 30 (1): 108-111. <http://dx.doi.org/10.13031/2013.30410>
- Montero J, Tarjuelo JM, Carrión P, 2003. Sprinkler droplet size distribution measured with an optical spectropluviometer. *Irrig Sci* 22 (2): 47-56. <http://dx.doi.org/10.1007/s00271-003-0069-3>
- Nuyttens D, Baetens K, Schampheleire MD, Sonck B, 2007. Effect of nozzle type, size and pressure on spray droplet characteristics. *Biosys Eng* 97 (3): 333-345. <http://dx.doi.org/10.1016/j.biosystemseng.2007.03.001>
- Salvador R, Bautista CC, Burguete J, Zapata N, Serreta A, Playan E, 2009. A photographic method for drop characterization in agricultural sprinklers. *Irrig Sci* 27(4): 307-317. <http://dx.doi.org/10.1007/s00271-009-0147-2>
- Solomon KH, Kincaid DC, Bezdek JC, 1985. Drop size distributions for irrigation spray nozzles. *T ASAE* 28(6): 1966-1974. <http://dx.doi.org/10.13031/2013.32550>
- Testik FY, Barros AP, 2007. Toward elucidating the microstructure of warm rainfall: a survey. *Rev Geophys* 45 (2): 2637-2655. <http://dx.doi.org/10.1029/2005RG000182>
- Thompson AL, James LG, 1985. Water droplet impact and its effect on infiltration. *T ASAE* 28 (5): 1506-1510. <http://dx.doi.org/10.13031/2013.32468>
- Thompson AL, Regmi TP, Ghidry F, Gantzer CJ, Hjelmfelt AT, 2001. Influence of kinetic energy on infiltration and erosion [C]. Soil erosion research for the 21st century. Proc Int Symp Honolulu, Hawaii, USA, January 3-5. Am Soc Agric Eng, pp: 151-154.
- Ulbrich CW, 1983. Natural variations in the analytical form of the raindrop size distribution. *J Climate Appl Meteor* 22 (10): 1764-1775. [http://dx.doi.org/10.1175/1520-0450\(1983\)022<1764:NVITAF>2.0.CO;2](http://dx.doi.org/10.1175/1520-0450(1983)022<1764:NVITAF>2.0.CO;2)
- Villiermaux E, Bossa B, 2009. Single-drop fragmentation determines size distribution of raindrops. *Nature Phys* 5 (9): 697-702. <http://dx.doi.org/10.1038/nphys1340>